

The foregoing results are clearly consistent with the rotational character of this nucleus, well established for the 0-5-MeV excitation region. They are also consistent with such an interpretation above this energy, including the first two  $T=\frac{3}{2}$  states first discussed on this basis by Morrison *et al.*<sup>5</sup> Whether the highest four levels discussed can be so interpreted is not clear at this time. It is also felt that our results indicate the potential usefulness of 180° electron scattering as a complement to other approaches in the investigation of rotational characteristics in odd-A nuclei.

*Note added in proof.* Recent threshold neutron work with the  $^{26}\text{Mg}(\gamma, n)^{26}\text{Mg}$  reaction by Berman, Baglin, and Bowman (unpublished) has come to our attention. With better energy resolution, their work suggests the

possibility that  $\Delta T=0$ ,  $M1$  transitions may be contributing to some of the peaks discussed as tentatively corresponding to  $T=\frac{3}{2}$  levels. There is reasonable evidence that this is not happening in the case of the 7.81-MeV peak. However, we cannot eliminate this possibility for peaks at greater excitation energies.

#### ACKNOWLEDGMENTS

We thank Susan Numrich for her help in the data accumulation and treatment. We are grateful to Dr. B. Chertok for communicating the DWBA results prior to publication. The cooperation of the NRL Linac operating staff is greatly appreciated. We also thank Professor H. Überall and Professor Stephen Shafroth for many helpful discussions.

### Study of the Low-Lying Excited States of $\text{Al}^{29}$ II: $\text{Al}^{27}(t, p\gamma)\text{Al}^{29}$ and $\text{Si}^{30}(t, \alpha\gamma)\text{Al}^{29}$ Angular Correlation Investigation\*

A. D. W. JONES, J. A. BECKER, AND R. E. McDONALD

Lockheed Palo Alto Research Laboratory, Palo Alto, California 94304

(Received 9 June 1969)

The low-lying excited states of  $\text{Al}^{29}$  have been investigated by measuring  $\gamma$ -ray angular correlations in a collinear geometry. The levels were populated in the  $\text{Al}^{27}(t, p\gamma)\text{Al}^{29}$  and  $\text{Si}^{30}(t, \alpha\gamma)\text{Al}^{29}$  reactions at triton bombarding energies of 2.8 and 2.5 MeV, respectively. The  $\gamma$ -ray branching ratios for states up to 3.7-MeV excitation energy were obtained. Spin assignments, or limits on the spins, for the first six excited states have been deduced on the basis of these data combined with previous results: [ $E_x, J^\pi$ ]; 1.40 MeV,  $\frac{1}{2}^+$ ; 1.76 MeV,  $(\frac{1}{2}, \frac{3}{2}, \frac{5}{2}, \frac{7}{2})$ ; 2.23 MeV,  $\frac{3}{2}, \frac{5}{2}, \frac{7}{2}$ ; 2.88 MeV,  $\frac{3}{2}^+, \frac{5}{2}^+$ ; 3.07 MeV,  $(\frac{3}{2}^+, \frac{5}{2}^+)$ ; and 3.19 MeV,  $(\frac{3}{2}, \frac{5}{2}^-, \frac{7}{2}^-, \frac{9}{2})$ .

#### I. INTRODUCTION

A RECENT investigation by Jones<sup>1</sup> of the differential cross section of the  $\text{Si}^{30}(t, \alpha)\text{Al}^{29}$  reaction at the incident triton energy  $E_t=11.8$  MeV has resulted in information on the states of  $\text{Al}^{29}$  up to 4.41-MeV excitation energy. The characteristic  $\alpha$ -particle angular distributions were interpreted to enable definite spin-parity assignments of  $J^\pi=\frac{1}{2}^+$  to be made to both the 1.402- and 3.434-MeV levels in  $\text{Al}^{29}$ . Restrictions were also placed on possible spin-parity values of several other levels. A summary of the available information on  $\text{Al}^{29}$  excited states, including these results, is presented in Ref. 1. In the present work,<sup>2</sup> further information on the excited states of  $\text{Al}^{29}$  is reported, *viz.*, the  $\gamma$ -ray branchings of low-lying levels with excitation energy  $E_x \leq 3.7$  MeV, and information about the spins and  $\gamma$ -ray transition multipolarities for states with  $E_x \leq 3.19$  MeV. These results were deduced from

measurements of  $\gamma$ -ray angular distributions from decaying residual nuclei aligned in a nuclear reaction.<sup>3</sup> States in  $\text{Al}^{29}$  were populated in both the  $\text{Al}^{27}(t, p\gamma)\text{Al}^{29}$  reaction ( $Q=8.68$  MeV) and the  $\text{Si}^{30}(t, \alpha\gamma)\text{Al}^{29}$  reaction ( $Q=6.22$  MeV), at bombarding energies of 2.8 and 2.5 MeV, respectively. The  $\gamma$ -ray angular distributions were obtained by measuring the yield of  $\gamma$  rays at angles between  $\theta_\gamma=0^\circ$  and  $90^\circ$  in coincidence with reaction produced protons—when investigating the  $\text{Al}^{27}(t, p\gamma)\text{Al}^{29}$  reaction—or  $\alpha$  particles when investigating the  $\text{Si}^{30}(t, \alpha\gamma)\text{Al}^{29}$  reaction. The reaction particles were detected in an annular counter located near  $180^\circ$  with respect to the incident beam direction. Because of the angular symmetry involved when the outgoing reaction particle is detected at  $180^\circ$ ,  $\gamma$  decays are observed from  $\text{Al}^{29}$  states with only magnetic substates  $|m|=\frac{1}{2}$  populated as a result of the  $\text{Si}^{30}(t, \alpha)\text{Al}^{29}$  reaction, while in contrast, substates with values of  $|m|$  from  $\frac{1}{2}$  through  $\frac{7}{2}$  can be populated in the  $\text{Al}^{27}(t, p)\text{Al}^{29}$  reaction. In practice, these results are modified to the extent that higher magnetic sub-

\* Research supported in part by the Office of Naval Research and in part by the Lockheed Independent Research Program.

<sup>1</sup> A. D. W. Jones, Phys. Rev. **180**, 997 (1969).

<sup>2</sup> Preliminary accounts of the work have previously been reported in Bull. Am. Phys. Soc. **13**, 674 (1968); **13**, 1372 (1968).

<sup>3</sup> A. E. Litherland and A. J. Ferguson, Can. J. Phys. **52**, 788 (1961).

states than  $\frac{1}{2}$  or  $\frac{7}{2}$ , respectively, can be populated because the particle detector is not a point counter at  $180^\circ$ .

The  $\gamma$ -ray distributions may then be analyzed<sup>3,4</sup> to determine  $\gamma$ -ray branching ratios, level spins, and  $\gamma$ -ray transition multipole mixtures. The analyses are independent of the reaction mechanism since the populations of the magnetic substates,  $P(m)$ , are treated as experimentally determined parameters. Thus, in principle, it is simple to deduce level spin and  $\gamma$ -ray multipole mixing information from the  $\gamma$ -ray angular correlations obtained from the  $Si^{30}(t, \alpha\gamma)Al^{29}$  reaction, whereas by contrast the analysis of the  $Al^{27}(t, p\gamma)Al^{29}$   $\gamma$ -ray angular correlations suffers from a lack of knowledge of the  $P(m)$ 's which introduces several additional parameters into the analysis. These extra parameters together with the generally featureless angular correlations measured in the  $Al^{27}(t, p\gamma)Al^{29}$  reaction have the consequence that comparison with the correlation formulas<sup>4</sup> to determine level spins and  $\gamma$ -ray multipole mixtures yields little information. The measured coincidence yields in the  $t, p\gamma$  work, however, were much higher than for the  $Si^{30}(t, \alpha\gamma)Al^{29}$  reaction, and we present in Sec. III  $\gamma$ -ray branching ratios based on the  $Al^{27}(t, p\gamma)Al^{29}$   $\gamma$ -ray angular correlation study. On the other hand, correlations measured following the  $Si^{30}(t, \alpha\gamma)Al^{29}$  reaction could readily be compared with the correlation equations to deduce level spins and multipole mixtures; these results are presented in Sec. IV. Despite the fact that, in principle, the unknowns in the analysis of the angular correlations following the  $t, \alpha\gamma$  case are only the spin of the state and the multipole mixing ratio,  $\delta$ , unambiguous spin assignments proved difficult because most of the angular correlations extracted involved transitions to the  $J^\pi = \frac{5}{2}^+$  ground state. Thus, one can not generally differentiate between angular distributions produced by  $J = \frac{3}{2}, \frac{5}{2},$  and  $\frac{7}{2}$  levels decaying to this  $J = \frac{5}{2}$  state.

In a forthcoming paper,<sup>5</sup> the results of measurements of the mean lifetime of several low-lying states of  $Al^{29}$  are presented and the information presently available on the nucleus is then collated and interpreted in terms of a unified nuclear model.

## II. EXPERIMENTAL METHOD

### A. Branching Ratio Determination Using the $Al^{27}(t, p\gamma)Al^{29}$ Reaction

The experimental studies were carried out with the Van de Graaff generator and tritium facility of the Lockheed Palo Alto Research Laboratory. A beam of 2.8-MeV tritons after momentum analysis was colli-

dated to a spot size  $1 \times 1$  mm and used to bombard a  $130 \mu\text{g}/\text{cm}^2$  self-supporting foil of aluminum. The transmitted beam was stopped in a Faraday cup 6.3 cm behind the target from which a measure of the total transmitted charge was obtained. The reaction protons were detected in an annular silicon solid-state detector located with its front face 3 cm from the target, resulting in detection of particles at angles between  $165^\circ$  and  $175^\circ$  to the incoming beam direction. Sufficient aluminum foil ( $20 \text{ mg}/\text{cm}^2$ ) was placed in front of the counter to prevent elastically scattered tritons, reaction deuterons, and reaction  $\alpha$  particles from being detected. A  $10.2 \times 10.2$ -cm NaI(Tl) scintillator located with its front face 8.8 cm from the target was used to detect  $\gamma$  radiation. The scintillator was mounted on a 10-cm photomultiplier tube, the whole assembly being shielded on the sides with 5-cm-thick Pb. The crystal could be rotated about a vertical axis through the target; data was taken at angles from  $0^\circ$  to  $90^\circ$  with respect to the incident beam direction.

A coincidence between the two detectors ( $2\tau = 4 \times 10^{-8}$  sec) results in the storage of pulse-height information from both the charged-particle detector and the NaI(Tl) detector. The two-parameter data are accumulated, as has been previously described,<sup>6,7</sup> with conventional modular electronics and dual 4096-channel analog-to-digital converters interfaced to an SEL 810A computer with auxiliary magnetic-tape storage.<sup>8</sup> Approximately  $4 \times 10^3$  words of core memory are available for display of any part or parts of the  $4096 \times 4096$  matrix, while the full data matrix is recorded on magnetic tape for subsequent data manipulations. The matrix of both real plus random and random particle- $\gamma$  coincident pulse heights is recorded simultaneously. The real-to-random ratio is usually better than 10:1 for a full energy absorption peak. The system has the advantage of almost unlimited memory storage and great flexibility in the subsequent off-line analysis.

### B. Angular Correlation Study Using the $Si^{30}(t, \alpha\gamma)Al^{29}$ Reaction

A  $100 \mu\text{g}/\text{cm}^2$  target of  $Si^{30}$  was fabricated by evaporating 95.55% enriched  $Si^{30}O_2$  mixed with tantalum powder from a tantalum boat onto a  $20 \mu\text{g}/\text{cm}^2$  carbon foil. The experimental setup was similar to that described in II A, except that in this case three  $10.2 \times 10.2$ -cm NaI(Tl) crystals, denoted as A, B, and C for identification purposes, were simultaneously used to detect  $\gamma$  radiation in coincidence with reaction  $\alpha$  particles. The two-parameter matrices arising from

<sup>6</sup> L. F. Chase, Jr., in *Nuclear Research with Low Energy Accelerators*, edited by D. M. Van Patter and J. B. Marion (Academic Press Inc., New York, 1967).

<sup>7</sup> J. A. Becker, in *Proceedings of Third Symposium on the Structure of Low-Medium Mass Nuclei*, edited by J. P. Davidson (Kansas University Press, Lawrence, 1968).

<sup>8</sup> R. A. Chalmers, IEEE Trans. Nucl. Sci. NS-16, 132 (1969).

<sup>4</sup> A. R. Poletti and E. K. Warburton, Phys. Rev. **137**, B595 (1965).

<sup>5</sup> A. D. W. Jones, J. A. Becker, R. E. McDonald, and A. R. Poletti, Phys. Rev. (to be published).

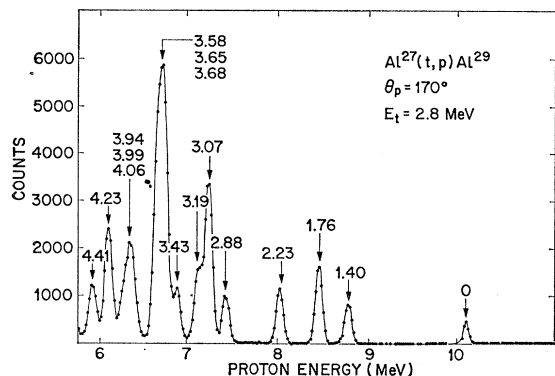


FIG. 1. Proton spectrum obtained at  $170^\circ$  laboratory angle from the  $\text{Al}^{27}(t, p)\text{Al}^{29}$  reaction at an incident triton energy of 2.8 MeV. The spectrum has chance coincidences subtracted out and the observed intensity of the ground-state group, which has been decreased by a factor of  $\sim 25$  from the true-plus-chance spectrum, is a measure of the efficiency of this process. The spectrum shows the protons in coincidence with  $\gamma$  rays of energy  $0.55 \leq E_\gamma \leq 4.5$  MeV, and is the result of summation of data accumulated at five  $\gamma$ -ray counter angles,  $\theta_\gamma = 0^\circ, 30^\circ, 45^\circ, 60^\circ,$  and  $90^\circ$ . Peaks in the spectrum corresponding to proton groups leaving the residual nucleus,  $\text{Al}^{29}$ , in its various excited states are labeled by the excitation energy of the level in MeV. The resolution is  $\sim 80$  keV for the particle peaks and arises primarily from the 20-mg/cm<sup>2</sup> aluminum foil placed in front of the counter to stop other reaction particles being detected.

coincidence events between each NaI(Tl) detector and the particle counter were stored separately by the data acquisition system.<sup>6-8</sup> One of the NaI(Tl) detectors (A) was rotated out of the horizontal plane  $\Phi_\gamma = 45^\circ$  and  $\theta_\gamma = 135^\circ$  with respect to the incoming beam direction. The front face of this detector was located 15 cm from the target. Coincident  $\alpha$ - $\gamma$  events obtained with this detector were used to monitor the reaction yield. Angular correlations were measured by rotating the other two crystals (B and C) in the horizontal plane  $\Phi_\gamma = 0^\circ$ , one on each side of the beam direction. Data were accumulated at angles of  $0^\circ, 30^\circ, 45^\circ, 60^\circ,$  and  $90^\circ$  with respect to the incident beam direction. The front face of these detectors was 8.8 cm from the reaction site. These latter two crystals were set up for convenience with the same electronic gain, and had the same amount of absorbing material between the target and crystals. The photopeak detection efficiency of these two crystals was equal within experimental errors, but consistent differences in the total count between these two detectors was found. This consistent difference was included as an efficiency correction, as necessary, when the total yield of  $\gamma$  rays measured in detectors B and C were fitted to the correlation formalism.<sup>4</sup>

### III. BRANCHING RATIO ANALYSIS AND RESULTS

Data reduction begins by obtaining from the two-parameter matrix the charged-particle spectrum that is coincident with  $\gamma$  rays in the energy interval  $0.55 \text{ MeV} \leq E_\gamma \leq 4.5 \text{ MeV}$ . Figure 1 shows such a distribution summed for 5 runs at  $\gamma$ -ray angles from  $0^\circ$

to  $90^\circ$ . In the singles spectrum observed at the same energy, the intensity of the ground-state group is  $\sim 12$  times greater than the 1.40-MeV strength to be compared with a ratio of 0.5 observed after subtraction of chance coincidences. The decrease in observed strength of the ground-state group is therefore a measure of the residual chance-coincidence contribution to the spectrum. The charged-particle resolution is 80 keV and is due mainly to the absorber placed in front of the detector. After the peaks are located and identified, the  $\gamma$ -ray pulse-height distribution coincident with the particle groups of interest is obtained, integrating over the charged-particle peak. Figures 2 and 3 illustrate  $\gamma$ -ray spectra obtained in this fashion. When the various groups in the charged-particle spectrum were either not resolved or only partially resolved,  $\gamma$ -ray decay modes were determined by examining adjacent intervals in the two-parameter matrix. For example, the triplet of levels at an excitation energy of 3.6 MeV is not resolved in the charged-particle spectrum; to extract the necessary information a two-parameter spectrum was set up including  $\gamma$  rays with  $E_\gamma \geq 100$  keV and protons of energies corresponding to this triplet. Branching modes could then be deduced by examination of the  $\gamma$ -ray spectra in coincidence with adjacent pulse-height regions of the particle spectrum. These data are shown in the upper half of Fig. 3.

Angular correlations of  $\gamma$  rays coincident with the appropriate proton group were extracted for all states up to an excitation energy of 3.68 MeV. The reaction yield was monitored by recording the particle spectrum on a TMC 1024-channel analyzer without imposing any coincident requirements. It was found that for all runs the total integrated charge and monitor counts

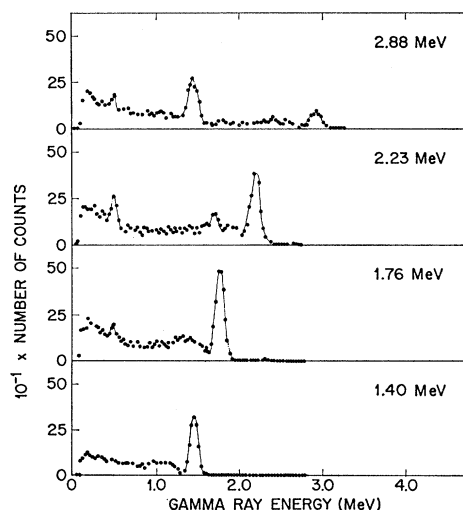


FIG. 2. Summed  $\gamma$ -ray spectra obtained in coincidence with the 1.40-, 1.76-, 2.23-, and 2.88-MeV proton groups in the  $\text{Al}^{27}(t, p\gamma)\text{Al}^{29}$  reaction. The spectra show real plus random coincidences. The  $\gamma$ -ray branching ratios of the states shown in Table II are obtained from these data.

TABLE I. Coefficients resulting from description of the  $Al^{27}(t, p\gamma)Al^{29}$  angular correlations in terms of a Legendre polynomial expansion.

$E_x$ (MeV)	$E_\gamma$ (MeV)	Assignment	$W(\theta) = 1 + A_2 P_2(\cos\theta)$		$W(\theta) = 1 + A_2 P_2(\cos\theta) + A_4 P_4(\cos\theta)$			
			$A_2$	Error	$A_2$	Error	$A_4$	Error
1.40	1.40	1.40→0	0.001	0.033	0.024	0.036	-0.064	0.039
1.76	1.76	1.76→0	0.028	0.023	0.033	0.025	-0.014	0.027
2.23	2.23	2.23→0	-0.077	0.033	-0.051	0.036	-0.058	0.037
2.88	2.88	2.88→0	-0.117	0.052	-0.079	0.057	-0.092	0.062
2.88	1.48 <sup>a</sup>	2.88→1.40	0.034	0.042	0.059	0.050	-0.073	0.050
	1.40	1.40→0						
3.07	3.07	3.07→0	-0.018	0.045	0.020	0.049	-0.096	0.054
3.07	1.31	3.07→1.76	-0.026	0.023	-0.012	0.025	-0.032	0.027
3.19	1.43	3.19→1.76	0.046	0.045	0.056	0.049	-0.027	0.056
3.19	0.96	3.19→2.23	0.001	0.039	0.002	0.045	0.008	0.054
3.43	2.03	3.43→1.40	0.048	0.088	0.063	0.095	-0.044	0.104
3.58	3.58	3.58→0	0.057	0.084	0.107	0.090	-0.144	0.093
3.58	1.82 <sup>a</sup>	3.58→1.76	-0.006	0.027	-0.022	0.029	0.039	0.028
	1.76	1.76→0						
3.65	3.65	3.65→0	-0.039	0.044	-0.052	0.045	0.041	0.044
3.65	1.89	3.65→1.76	-0.014	0.017	0.002	0.018	-0.048	0.020
	1.76	1.76→0						
3.68	3.68	3.68→0	-0.040	0.026	-0.029	0.029	-0.027	0.031

<sup>a</sup>  $\gamma$  rays not resolved. Sum of both was fitted to the Legendre polynomial expansion.

in the particle group corresponding to the 1.40-MeV state agreed within statistical errors; hence the data taken were normalized to the average of these. The angular correlations show no large anisotropies, and we show in Fig. 4 as typical those obtained for the  $\gamma$  decay of the 1.40-, 1.76-, and 2.23-MeV states. Expansion coefficients resulting from a least-squares fit of these angular correlations to a Legendre polynomial expansion of the form

$$W(\theta) = I_\gamma (1 + A_2 P_2(\cos\theta) + A_4 P_4(\cos\theta)) \quad (1)$$

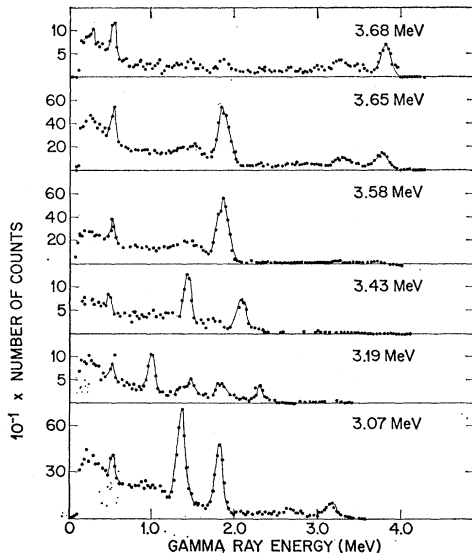


FIG. 3. Summed  $\gamma$ -ray spectra obtained in coincidence with the 3.07-, 3.19-, 3.43-, 3.58-, 3.65-, and 3.68-MeV proton groups. The data for the 3.58-, 3.65-, and 3.68-MeV states were obtained by taking successive sections of the particle group shown in Fig. 1 and observing the  $\gamma$  rays in coincidence with all sections.

are given in Table I. From data such as these and from NaI(Tl) efficiency curves,<sup>9</sup> the  $\gamma$ -ray branching ratios summarized in Table II were deduced. The quoted results have been corrected for solid-angle addition of the  $\gamma$ -ray pulses in the case of cascade and cross-over transitions. For comparison, we also show in Table II some other recent results<sup>10,11</sup> on the branchings of the  $Al^{29}$  levels. The agreement, in general, is good. We

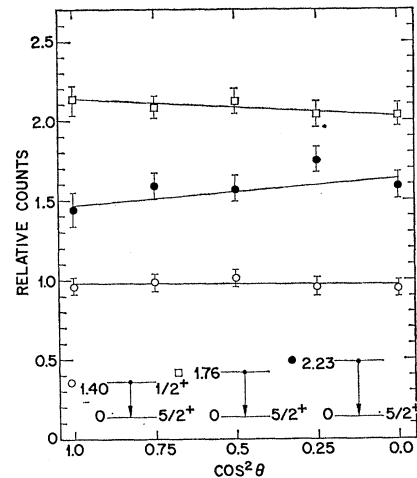


FIG. 4. Angular correlations for the 1.40-, 1.76-, and 2.23-MeV  $\gamma$  rays obtained from the  $Al^{27}(t, p\gamma)Al^{29}$  reaction. The isotropy of the 1.40-MeV  $\gamma$  ray is consistent with the  $J^\pi = \frac{1}{2}^+$  assignment to this level.

<sup>9</sup> K. Coop and H. A. Grench, Nucl. Instr. Methods **36**, 339 (1965).

<sup>10</sup> D. C. Kean, K. W. Carter, and R. H. Spear, Nucl. Phys. **A123**, 430 (1969).

<sup>11</sup> R. G. Hirko, Bull. Am. Phys. Soc. **13**, 1371 (1968); (private communication).

TABLE II.  $\gamma$ -ray branching ratios for the levels of  $\text{Al}^{29}$  with  $E_x < 3.7$  MeV.

$E_i$ (MeV)	$E_f$ (MeV)	$E_\gamma$ (MeV)	Branching ratios (%)			$E_i$ (MeV)	$E_f$ (MeV)	$E_\gamma$ (MeV)	Branching ratios (%)				
			Present work	Other <sup>a</sup>	Other <sup>b</sup>				Present work	Other <sup>a</sup>	Other <sup>b</sup>		
1.402	0	1.402	100					3.071	0.363	<3	<9		
1.762	0	1.762	100	100	>98			3.191	0.243	<14	<7		
	1.402	0.360	<1	<5				3.584	0	3.584	14±2	21±2	14±4
2.228	0	2.228	100	99±1	>95			1.402	2.182	<3	<5		
	1.402	1.826	<1	1±1				1.762	1.822	86±2	79±3	86±4	
	1.762	1.466	<4	<3				2.228	1.356	<3	<3		
2.875	0	2.875	56±2	67±2	58±2			2.875	0.709	<4	<4		
	1.402	1.473	44±2	33±1	42±2			3.071	0.513	<7	<5		
	1.762	1.113	<2	<4				3.191	0.393	<2	<6		
	2.228	0.647	<2	<2				3.434	0.150	<3	<6		
3.071	0	3.071	29±2	40±2	33±4			3.646	0	3.646	56±3		83±12
	1.402	1.669	<4	<7				1.402	2.244	<3			
	1.762	1.309	71±2	58±2	67±4			1.762	1.884	44±3		17±12	
	2.228	0.843	<5	2±2				2.228	1.418	<3		(<13)	
	2.875	0.196	<4	<6				2.875	0.771	<2			
3.191	0	3.191	10±3	15±2	6±2			3.071	0.575	<6			
	1.402	1.789	<10 <sup>e</sup>		9±6			3.191	0.455	<4			
	1.762	1.429	25±7	33±2 <sup>d</sup>	29±3			3.434	0.212	<4			
	2.228	0.963	65±7	52±1	56±5			3.584	0.062	...			
	2.875	0.316	<5	<10				3.676	0	3.676	100		(100)
3.434	0	3.434	6±2	16±4	<15			1.402	2.274	<15			
	1.402	2.032	74±3	69±3	71±5			1.762	1.914	<4			
	1.762	1.672	<9	<5				2.228	1.448	<15		(<13)	
	2.228	1.206	20±3	15±2	29±5			2.875	0.801	<5			
	2.875	0.559	<9	<4				3.071	0.605	<4			
								3.191	0.485	<22			
							3.434	0.242	<4				
							3.584	0.092	<15				

<sup>a</sup> Reference 10. The errors quoted do not include a possible  $\pm 15\%$  error due to anisotropies of the angular correlations (see text of Ref. 10).

<sup>b</sup> Reference 11.

<sup>c</sup> A better limit,  $<6\%$ , has been placed on the 3.19→1.40 branch in a subsequent experiment employing a Ge(Li)  $\alpha$ -ray spectrometer.

<sup>d</sup> Reference 13. Observed decay goes to the 1.76-MeV state and not 1.40-MeV state.

TABLE III. Legendre polynomial expansion coefficients of the  $\text{Si}^{30}(t, \alpha\gamma)\text{Al}^{29}$   $\gamma$ -ray angular correlations.

$E_x$ (MeV)	$E_\gamma$ (MeV)	Assignment	$W(\theta) = 1 + A_2 P_2(\cos\theta)$		$W(\theta) = 1 + A_2 P_2(\cos\theta) + A_4 P_4(\cos\theta)$			
			$A_2$	Error	$A_2$	Error	$A_4$	Error
1.40	1.40	1.40→0	0.001	0.014	0.003	0.014	-0.008	0.017
1.76	1.76	1.76→0	0.040	0.027	0.033	0.030	-0.017	0.031
2.23	2.23	2.23→0	0.164	0.027	0.160	0.029	0.012	0.032
2.88	2.88	2.88→0	-0.262	0.040	-0.296	0.044	0.089	0.046
2.88	1.48	2.88→1.40 <sup>a</sup>	-0.294	0.050	-0.288	0.056	-0.108	0.058
3.07	3.07	3.07→0	-0.033	0.047	0.014	0.058	-0.081	0.059
3.07	1.31	3.07→1.76	-0.210	0.034	-0.214	0.042	0.007	0.045
3.07	1.76	1.76→0	-0.008	0.032	-0.018	0.036	0.025	0.040
3.19	0.96	3.19→2.23	-0.280	0.068	-0.264	0.076	-0.034	0.084
3.19	2.23	2.23→0	0.119	0.045	0.125	0.049	-0.016	0.055
3.19	1.43	3.19→1.76	-0.280	0.075	-0.238	0.082	-0.095	0.091
3.19	1.76	1.76→0	0.179	0.071	0.156	0.078	0.074	0.090

<sup>a</sup> The isotropic component of the unresolved 1.40→0 transition was subtracted before data analysis was carried out.

have summarized these data in Fig. 5, which shows a partial level scheme for  $Al^{29}$ . The excitation energies of the levels are from the work of Jaffe *et al.*<sup>12</sup>

#### IV. $Si^{30}(t, \alpha\gamma)^{29}$ ANGULAR CORRELATIONS AND ANALYSIS

In a similar fashion, as in Sec. III above, the yields of the  $\gamma$ -ray components for  $Al^{29}$  levels with  $E_x \leq 3.19$  MeV were extracted. The  $\alpha$ -particle spectrum obtained in coincidence with  $\gamma$  rays of energy  $0.55 < E_\gamma < 4.0$  MeV in NaI(Tl) crystal B is shown in Fig. 6. The spectrum is obtained after subtraction of events due to random coincidences and is the result of five runs with the  $\gamma$ -ray counter at angles  $0^\circ, 30^\circ, 45^\circ, 60^\circ,$  and

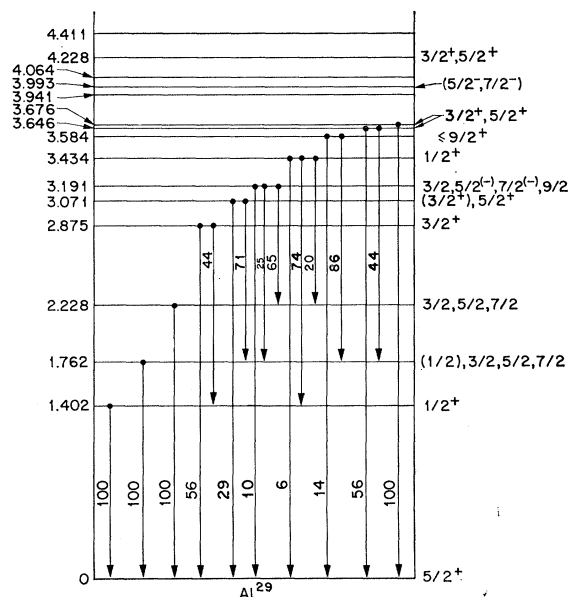


FIG. 5. Partial energy level diagram for  $Al^{29}$ . The level energies are obtained from the work of Jaffe *et al.* (Ref. 12) except for the 2.228-MeV level, which is as quoted by Barse *et al.* [Phys. Rev. **167**, 1043 (1968)]. The  $\gamma$ -decay of the levels is obtained from the present work and the spin-parity assignments are from Ref. 1 and the present work.

$90^\circ$ . After normalization to the reaction yield and the total efficiencies of detectors B and C, these yields were fitted to the Legendre polynomial expansion of Eq. (1). The resulting expansion coefficients for the 12  $\gamma$ -ray angular correlations extracted from these data are summarized in Table III. These coefficients are not corrected for finite counter acceptance angle. Typical values of these are  $Q_2=0.86, Q_4=0.60$  for a 1.5-MeV  $\gamma$  ray. In general, while the correlations are stronger than found for the  $Al^{27}(t, p\gamma)Al^{29}$  study, no distribution required a  $P_4(\cos\theta)$  term in the expansion for a satisfactory fit. The measured angular correlations were then fitted to theoretical formulas as

<sup>12</sup> A. A. Jaffe, F. DeS. Barros, P. D. Forsyth, J. Muto, I. J. Taylor, and S. Ramavataram, Proc. Phys. Soc. (London) **76**, 914 (1960).

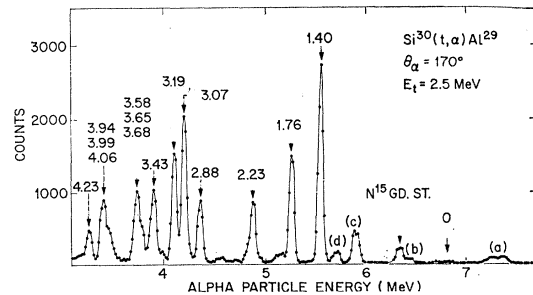


FIG. 6.  $\alpha$ -particle spectrum obtained at  $170^\circ$  laboratory angle from the  $Si^{30}(t, \alpha)Al^{29}$  reaction at 2.5 MeV. The spectrum has random coincidences subtracted out and shows the  $\alpha$  particles in coincidence with  $\gamma$  rays of energy  $0.55 \leq E_\gamma \leq 4.5$  MeV. Peaks in the spectrum corresponding to proton groups leaving the residual nucleus  $Al^{27}$  in its various excited states are labeled by the excitation energy, in MeV, of the level. The  $\alpha$ -particle group marked (a) contains counts arising from the  $Si^{28}(t, \alpha)Al^{27}$  reaction to the 0, 0.86-, and 1.01-MeV states in  $Al^{27}$ . These arise from the 4%  $Si^{28}$  impurity in the target. Groups (b), (c), and (d) are attributed to the  $Al^{27}$  2.21-MeV level, 2.73-MeV level, and 3.00-MeV doublet, respectively. Other higher excited states of  $Al^{27}$  are observed in the spectrum, but they provide no major problem in the analysis until  $\alpha$ -particle energies less than 4 MeV are considered.

previously described.<sup>4</sup> In all these fits the spin of the ground state of  $Al^{29}$  was taken to be  $J=\frac{5}{2}$  and for the 1.40-MeV state  $J=\frac{1}{2}$ . For the excited states, assumed spins of  $J=\frac{1}{2}, \frac{3}{2}, \frac{5}{2}, \frac{7}{2},$  and  $\frac{9}{2}$  were taken in turn. Spins  $J \geq \frac{1}{2}$  were not considered in the analysis. The justification for this step lies in the measured<sup>5</sup> mean lifetimes of the states with  $E_x \leq 3.2$  MeV. These levels—with the exception of the 1.40-MeV state whose spin is known to be  $J=\frac{1}{2}$ —have  $\tau_m < 10^{-12}$  sec. From the

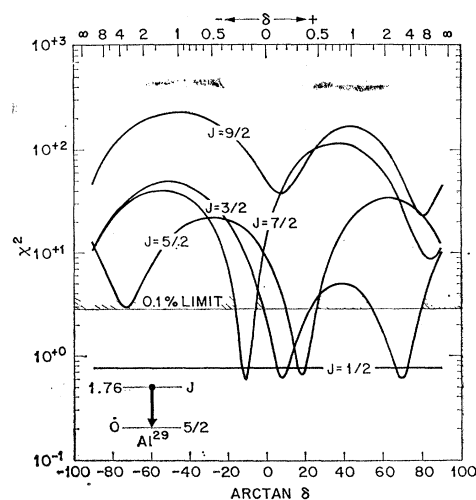


FIG. 7.  $\chi^2$  against  $\tan^{-1}\delta$  plot for the 1.76-MeV  $\gamma$  ray. For each assumed spin value for the 1.76-MeV state the angular distribution of the  $\gamma$  ray is calculated for values of  $\delta$  between  $-\infty$  and  $\infty$ . A least-squares comparison with the measured correlation is then made. In this and succeeding fits possible spin values are assigned to a level if  $\chi^2$  falls below the 0.1% confidence limit as obtained from standard  $\chi^2$  tables. The error on the mixing ratio thus determined is obtained at the 0.1% confidence limit. In these calculations, the finite size of the particle counter is taken into consideration as discussed in the text.

TABLE IV. Allowed spin values and mixing ratios.

$E_x$ (MeV)	Transition	$J_i$	$J_{int}$	$J_f$	$\delta$	$\chi^2$	$E_x$ (MeV)	Transition	$J_i$	$J_{int}$	$J_f$	$\delta$	$\chi^2$
1.76	1.76→0	$\frac{1}{2}$	...	$\frac{5}{2}$	Undetermined	0.68	3.19	3.19→1.76→0	$\frac{3}{2}$	$\frac{1}{2}$	$\frac{5}{2}$	$-0.05_{-0.41}^{+0.29}$	0.88
		$\frac{3}{2}$	...	$\frac{5}{2}$	$+0.14_{-0.18}^{+0.26}$	0.60			$\frac{3}{2}$	$\frac{3}{2}$	$\frac{5}{2}$	$2.05_{-1.2}^{+3.1}$	0.88
		$\frac{5}{2}$	...	$\frac{5}{2}$	$+2.75_{-1.27}^{+2.92}$	0.60			$\frac{3}{2}$	$\frac{5}{2}$	$\frac{5}{2}$	$\geq 0.16; \leq -11.4$	0.89
		$\frac{7}{2}$	...	$\frac{5}{2}$	$+0.34 \pm 0.15$	0.68			$\frac{3}{2}$	$\frac{7}{2}$	$\frac{5}{2}$	$\geq 2.1; \leq 0.27$	0.82
2.23	2.23→0	$\frac{3}{2}$	...	$\frac{5}{2}$	$-0.19_{-0.08}^{+0.09}$	0.57	$\frac{5}{2}$	$\frac{3}{2}$	$\frac{5}{2}$	$\geq 1.4; \leq 0.17$	0.88		
		$\frac{5}{2}$	...	$\frac{5}{2}$	$0.11 \leq \delta \leq 2.99$	0.58	$\frac{5}{2}$	$\frac{5}{2}$	$\frac{5}{2}$	$-0.17_{-0.29}^{+0.25}$	0.80		
		$\frac{7}{2}$	...	$\frac{5}{2}$	$\chi_{min}^2$ at $\delta = 0.33$ or 1.63		$\frac{5}{2}$	$\frac{7}{2}$	$\frac{5}{2}$	$2.60_{-1.0}^{+2.1}$	1.6		
		$\frac{9}{2}$	...	$\frac{5}{2}$	$0.21_{-0.16}^{+0.15}$	0.60	$\frac{5}{2}$	$\frac{9}{2}$	$\frac{5}{2}$	$\geq 0.25; \leq -2.6$	0.80		
2.88	2.88→0	$\frac{3}{2}$	...	$\frac{5}{2}$	$-2.45_{-0.43}^{+0.34}$	2.40	$\frac{7}{2}$	$\frac{3}{2}$	$\frac{5}{2}$	$-0.14_{-0.44}^{+0.35}$	0.82		
		$\frac{5}{2}$	...	$\frac{5}{2}$	$-0.27_{-0.10}^{+0.11}$	0.57	$\frac{7}{2}$	$\frac{5}{2}$	$\frac{5}{2}$	$\geq 3.3; \leq -2.3$	0.82		
		$\frac{7}{2}$	...	$\frac{5}{2}$	$-0.24_{-0.24}^{+0.27}$	0.80	$\frac{7}{2}$	$\frac{7}{2}$	$\frac{5}{2}$	$0.36_{-0.17}^{+0.21}$	1.8		
2.88	2.88→1.40	$\frac{3}{2}$	...	$\frac{1}{2}$	$\geq 4.3; \leq -3.7$	0.80	$\frac{9}{2}$	$\frac{3}{2}$	$\frac{5}{2}$	$1.96_{-0.68}^{+1.12}$	1.8		
		$\frac{5}{2}$	...	$\frac{1}{2}$	$0.0 \pm 0.21$	0.68	$\frac{9}{2}$	$\frac{5}{2}$	$\frac{5}{2}$	$0.0 \pm 0.27$	0.80		
3.07	3.07→0	$\frac{3}{2}$	...	$\frac{5}{2}$	$1.80_{-0.71}^{+1.27}$	0.68	$\frac{9}{2}$	$\frac{7}{2}$	$\frac{5}{2}$	$3.1_{-1.2}^{+3.2}$	1.60		
		$\frac{5}{2}$	...	$\frac{5}{2}$	$0.05_{-0.26}^{+0.37}$	0.28	$\frac{9}{2}$	$\frac{9}{2}$	$\frac{5}{2}$	$\geq 0.33; \leq -1.80$	0.80		
		$\frac{7}{2}$	...	$\frac{5}{2}$	$3.7_{-2.2}^{+15.4}$	0.28	$\frac{9}{2}$	$\frac{9}{2}$	$\frac{5}{2}$	$0.36_{-0.21}^{+0.34}$	1.60		
3.07	3.07→1.76→0	$\frac{5}{2}$	...	$\frac{5}{2}$	$0.41_{-0.23}^{+0.26}$	0.18	$\frac{9}{2}$	$\frac{7}{2}$	$\frac{5}{2}$	$2.48_{-1.28}^{+3.50}$	1.40		
		$\frac{7}{2}$	...	$\frac{5}{2}$	$-3.7_{-7.7}^{+1.9}$	0.33	$\frac{9}{2}$	$\frac{9}{2}$	$\frac{5}{2}$	$0.0_{-0.23}^{+0.27}$	0.82		
		$\frac{9}{2}$	...	$\frac{5}{2}$	$-0.11_{-0.14}^{+0.13}$	0.77	$\frac{9}{2}$	$\frac{9}{2}$	$\frac{5}{2}$	$3.5_{-1.4}^{+4.1}$	1.60		
		$\frac{11}{2}$	...	$\frac{5}{2}$	$+2.36_{-0.70}^{+1.13}$	0.77	$\frac{9}{2}$	$\frac{9}{2}$	$\frac{5}{2}$	$0.23 \leq \delta \leq 5.7$	1.3		
		$\frac{13}{2}$	...	$\frac{5}{2}$	$0.50_{-0.22}^{+0.34}$	0.77	$\frac{9}{2}$	$\frac{9}{2}$	$\frac{5}{2}$	$-0.25_{-0.75}^{+0.41}$	1.0		
		$\frac{15}{2}$	...	$\frac{5}{2}$	$5.14_{-3.0}^{+33.0}$	0.77	$\frac{9}{2}$	$\frac{9}{2}$	$\frac{5}{2}$	$\geq 3.25; \leq -1.7$	1.0		
		$\frac{17}{2}$	...	$\frac{5}{2}$	$-0.16 \pm 0.22$	0.80	$\frac{9}{2}$	$\frac{9}{2}$	$\frac{5}{2}$	$\geq 2.1; \leq 0.09$	1.1		
		$\frac{19}{2}$	...	$\frac{5}{2}$	$\geq 3.7; \leq -6.7$	0.80	$\frac{9}{2}$	$\frac{9}{2}$	$\frac{5}{2}$	$-0.02 \pm 0.21$	1.1		
		$\frac{21}{2}$	...	$\frac{5}{2}$	$-0.42_{-0.25}^{+0.32}$	0.80	$\frac{9}{2}$	$\frac{9}{2}$	$\frac{5}{2}$	$2.00_{-0.12}^{+1.73}$	1.7		
		$\frac{23}{2}$	...	$\frac{5}{2}$	$\geq 2.2; \leq -38.0$	0.80	$\frac{9}{2}$	$\frac{9}{2}$	$\frac{5}{2}$	$\geq 0.33; \leq -3.7$	1.1		
3.07	3.07→1.76→0	$\frac{25}{2}$	...	$\frac{5}{2}$	$-0.07 \pm 0.10$	0.82	$\frac{9}{2}$	$\frac{9}{2}$	$\frac{5}{2}$	$-0.12_{-0.28}^{+0.37}$	1.0		
		$\frac{27}{2}$	...	$\frac{5}{2}$	$+0.63_{-0.22}^{+0.34}$	0.88	$\frac{9}{2}$	$\frac{9}{2}$	$\frac{5}{2}$	$\geq 4.0; \leq -3.1$	1.0		
		$\frac{29}{2}$	...	$\frac{5}{2}$	$\geq 16.4; \leq -4.7$	0.88	$\frac{9}{2}$	$\frac{9}{2}$	$\frac{5}{2}$	$0.0 \pm 0.19$	1.1		
		$\frac{31}{2}$	...	$\frac{5}{2}$	$-0.08_{-0.16}^{+0.14}$	0.80	$\frac{9}{2}$	$\frac{9}{2}$	$\frac{5}{2}$	$3.1_{-0.8}^{+1.6}$	1.8		
$\frac{33}{2}$	...	$\frac{5}{2}$	$\geq 5.4; \leq -9.5$	0.80	$\frac{9}{2}$	$\frac{9}{2}$	$\frac{5}{2}$	$\geq 0.40; \leq -2.25$	1.1				
$\frac{35}{2}$	...	$\frac{5}{2}$				$\frac{9}{2}$	$\frac{9}{2}$	$\frac{5}{2}$	$0.0 \pm 0.19$	1.1			
$\frac{37}{2}$	...	$\frac{5}{2}$				$\frac{9}{2}$	$\frac{9}{2}$	$\frac{5}{2}$	$3.5_{-1.1}^{+2.8}$	1.8			

known  $\gamma$ -ray decay of these states, and from compilations of systematics of  $\gamma$ -ray multiplicities—which indicate the largest probable transition strength for a given multipolarity—we can rule out  $J \geq \frac{1}{2}$  for any of the states under consideration with a high degree of confidence.

Results obtained for each state are presented below.

**1.40-MeV level.** This level is known<sup>1</sup> to have a spin-parity value of  $\frac{1}{2}^+$ . The extracted angular correlation is isotropic (see Table III), consistent with this assignment. The isotropy of this line ( $A_2 = 0.00 \pm 0.01$ ) was taken as evidence for the correct alignment of the goniometer.

**1.76-MeV level.** This level decays  $\geq 99\%$  to the ground state (see Table II). The angular correlation of the 1.76-MeV  $\gamma$  ray is isotropic within experimental error,  $A_2 = 0.03 \pm 0.03$ . In Fig. 7, we show plots of  $\chi^2$  the goodness of fit parameter [Eq. (14), Ref. 4] versus  $\tan^{-1}\delta$ , where  $\delta$  is the multipole mixing ratio for the 1.76-MeV  $\gamma$  ray, for various assumed spins of the 1.76-MeV level. We see that spins of  $\frac{1}{2}$ ,  $\frac{3}{2}$ ,  $\frac{5}{2}$ , and  $\frac{7}{2}$

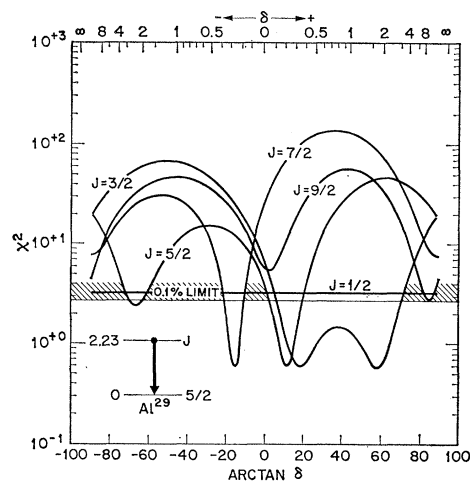


FIG. 8.  $\chi^2$  against  $\tan^{-1}\delta$  for the 2.23-MeV  $\gamma$  ray. Similar considerations apply as shown in the caption to Fig. 7.

are consistent with these data; that is, values of  $\chi^2$  below the 0.1% confidence limit are obtained for these spins, while  $J = \frac{9}{2}$  is ruled out because of the large  $\chi^2$  obtained for all possible values of  $\delta$ . The calculations shown in Fig. 7 were all carried out allowing for the fact that the  $\alpha$  counter was not a point detector at  $180^\circ$  and that population of magnetic substates  $P(m)$  with  $|m| > \frac{1}{2}$  is possible. In these calculations this finite-size effect (FSE) was taken into consideration by allowing magnetic substates with  $|m| = \frac{3}{2}$  to be populated to the extent of 10% of the  $|m| = \frac{1}{2}$  substate.<sup>4</sup> For every allowed  $J$ , possible values of the mixing ratios are shown in Table IV. Mixing ratios shown in this table in this case, as well as for the other levels discussed below, were obtained with a

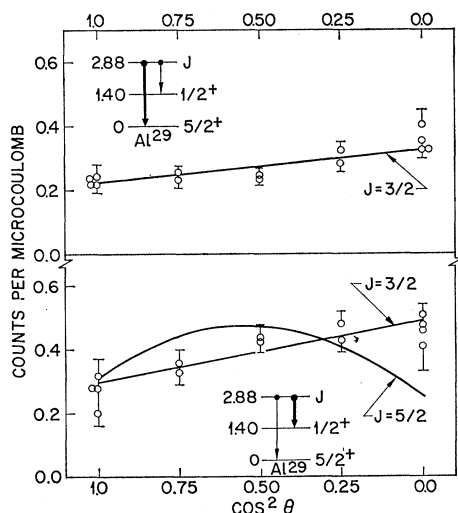


FIG. 9. Angular correlation of  $\gamma$  rays deexciting the 2.88-MeV state. Shown as a fit to the 2.88 $\rightarrow$ 0 correlation is the best fit with  $J = \frac{3}{2}$  evaluated at the minimum of the  $\chi^2$  curve shown in Fig. 11. For the 2.88 $\rightarrow$ 1.40 transition the best  $J = \frac{3}{2}$  fit evaluated at the minimum of  $\chi^2$  shown in Fig. 10 is drawn. The  $J = \frac{5}{2}$  fit also shown is the best fit found for this spin value.

10% FSE included in the calculations. The error limits on the mixing ratios were taken at the 0.1% confidence limit.

Previous information on the spin parity of this state has been obtained in the  $\text{Si}^{30}(t, \alpha)\text{Al}^{29}$  direct reaction investigation.<sup>1</sup> The  $\alpha$ -particle angular distribution to this state did not show a pattern characteristic of a direct reaction. Assuming, however, that the state was populated by a compound-nucleus process the experimental evidence suggested  $J = \frac{5}{2}$  for the 1.76-MeV level.

**2.23-MeV level.** The decay of this level is  $>95\%$  to the ground state. From Table III, the observed angular correlation of the 2.23-MeV  $\gamma$  ray is characterized by  $A_2 = 0.16 \pm 0.03$ . In Fig. 8, we show a  $\chi^2$  versus  $\tan^{-1}(\delta)$  plot. We see that for spins  $J = \frac{3}{2}$ ,  $\frac{5}{2}$ , and  $\frac{7}{2}$ , the curve falls below the 0.1% confidence limit but that  $J = \frac{1}{2}$  and  $\frac{9}{2}$  are excluded. Again the fits

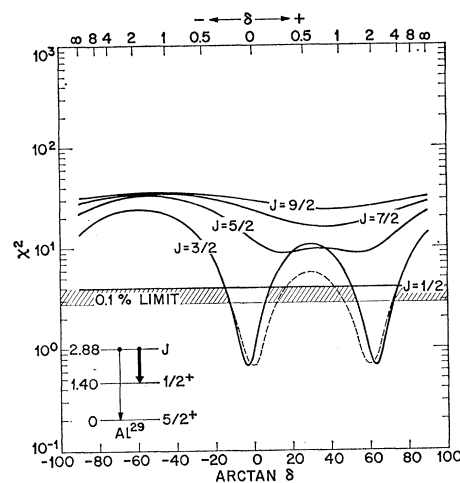


FIG. 10.  $\chi^2$  versus  $\tan^{-1}\delta$  for the 2.88 $\rightarrow$ 1.40 transition. Similar considerations apply as shown in the caption to Fig. 7. However, in this case the solid lines are calculations assuming a point counter at  $180^\circ$ . The effect of finite size of the counter is shown by the dotted line for the  $J = \frac{3}{2}$  fit only. This calculation allowed the magnetic substates with  $m = \pm \frac{3}{2}$  to be populated to the extent of 10% of the  $m = \pm \frac{1}{2}$  substate. The mixing ratio quoted in Table IV is obtained from the calculation that includes the finite-size effect.

shown include a 10% FSE. The allowable mixing ratios are given in Table IV. Like the 1.76-MeV state, the 2.23-MeV level does not show a direct reaction pattern in the  $\text{Si}^{30}(t, \alpha)\text{Al}^{29}$  investigation at  $E_t = 11.8$  MeV; the analysis based on compound-nucleus assumptions suggested the spin  $J = \frac{3}{2}$ .

**2.88-MeV level.** This level decays 56% to the  $J = \frac{5}{2}$  ground state and 44% to the  $J = \frac{1}{2}$  state at 1.40 MeV; the angular correlations of both these  $\gamma$  rays is shown in Fig. 9. The 2.88 $\rightarrow$ 1.40 correlation requires  $J = \frac{3}{2}$  for the 2.88-MeV level, as illustrated by the  $\chi^2$  plots of Fig. 10. The  $\chi^2$  fits illustrated by the solid line in

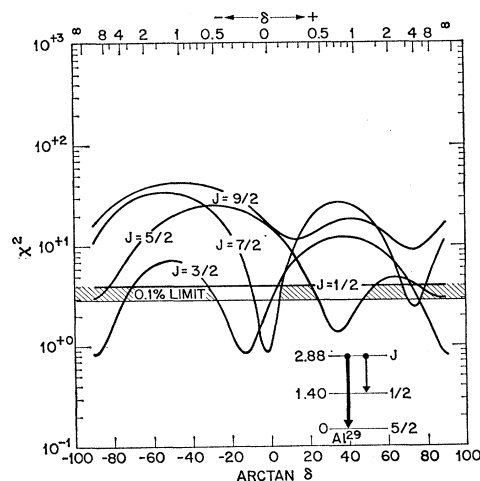


FIG. 11.  $\chi^2$  versus  $\tan^{-1}\delta$  for the 2.88 $\rightarrow$ 0 transition. Similar considerations apply as shown in the caption to Fig. 7.

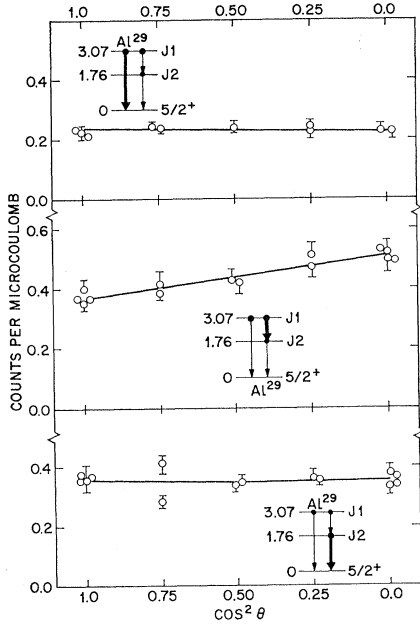


FIG. 12. The angular correlation of  $\gamma$  rays arising from the deexcitation of the 3.07-MeV level. The fits shown to the 3.07 $\rightarrow$ 1.76 transition is the best fit with  $J = \frac{3}{2}$  and  $\frac{5}{2}$  (indistinguishable) evaluated at the respective minima of the  $\chi^2$  curves shown in Fig. 13. The fits to the 3.07 $\rightarrow$ 1.76 and 1.76 $\rightarrow$ 0 transitions are the result of making a least-squares fit of the coefficients of Eq. (1) to the data. The coefficients deduced are shown in Table III.

Fig. 10 do not include any FSE contribution but the effect of its presence is shown on the  $J = \frac{3}{2}$  curve by the dotted line. Figure 11 illustrates the  $\chi^2$  plots for the 2.88 $\rightarrow$ 0 transition. The angular correlations calculated with  $J(2.88) = \frac{3}{2}$  and the mixing ratio taken at the minimum of the  $\chi^2$  curve are shown in Fig. 9 together

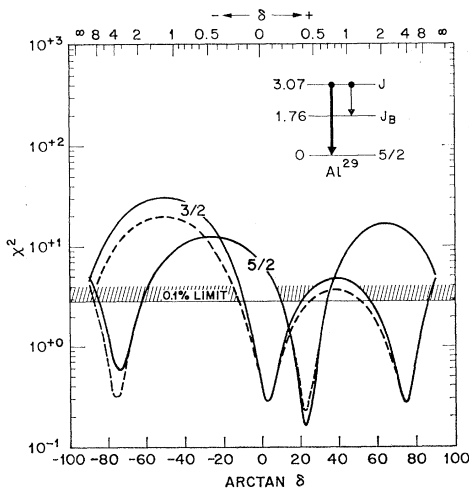


FIG. 13.  $\chi^2$  versus  $\tan^{-1}\delta$  for the 3.07 $\rightarrow$ 0 transition. See caption of Fig. 7 for details. The only spin values assumed for the 3.07-MeV state were  $J = \frac{3}{2}$  and  $\frac{5}{2}$ . The continuous lines are the results of calculations carried out without any finite-size considerations. The effect of a 10% population of the magnetic substates with  $m = \pm \frac{3}{2}$  is shown by the dotted lines.

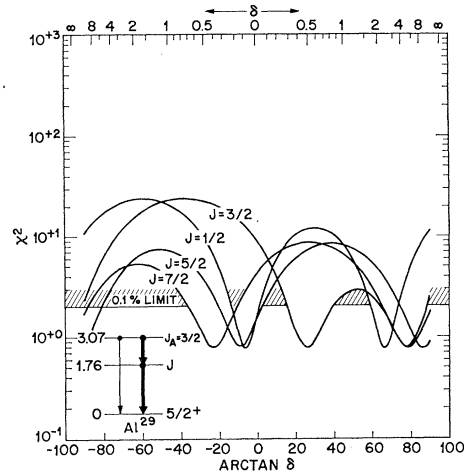


FIG. 14.  $\chi^2$  versus  $\tan^{-1}\delta$  for the 3.07 $\rightarrow$ 1.76-MeV transitions. The spin of the 3.07-MeV level is fixed as  $\frac{3}{2}$ , and the various  $J$  values shown in the diagram are for the 1.76-MeV level. The 3.07 $\rightarrow$ 1.76 and 1.76 $\rightarrow$ 0 correlations were simultaneously fitted, with the mixing ratios previously determined for the latter transition being fed into our calculations. All curves shown include a 10% finite-size effect.

with the best correlation resulting from a  $J = \frac{5}{2}$  assignment for comparison. Previous work<sup>1</sup> on the 2.88-MeV state results in  $J^\pi = \frac{3}{2}^+$  or  $\frac{5}{2}^+$ ; we are now in a position to make an unambiguous  $J^\pi = \frac{3}{2}^+$  assignment.

**3.07-MeV level.** The  $\gamma$ -ray angular correlations obtained for the decay of this level are shown in Fig. 12. Previous work<sup>1</sup> has shown that this state has  $J^\pi$  of either  $\frac{3}{2}^+$  or  $\frac{5}{2}^+$ , and our analysis of the correlation is restricted to these two alternatives. An analysis of the 3.07 $\rightarrow$ 0 transition reveals acceptable fits for both spin values with the E2/M1 mixing ratios shown in Table IV. The  $\chi^2$  versus  $\tan^{-1} \delta$  plots are shown in Fig. 13.

The results of simultaneously fitting the 3.07 $\rightarrow$ 1.76 $\rightarrow$

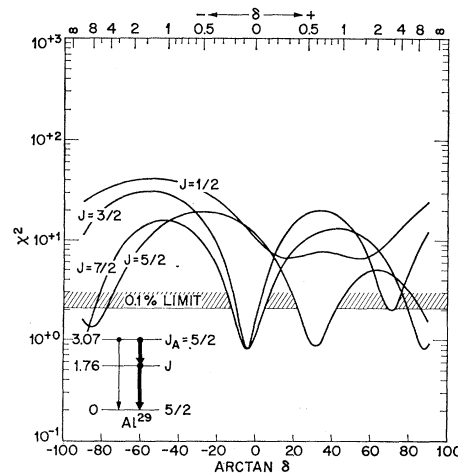


FIG. 15.  $\chi^2$  versus  $\tan^{-1}\delta$  for the 3.07 $\rightarrow$ 1.76 MeV transition. Calculations and considerations similar to Fig. 14 except that the spin of the 3.07-MeV level is fixed at  $J = \frac{5}{2}$ .

0 transitions are shown in Figs. 14 and 15 for assumed spins  $J = \frac{1}{2}, \frac{3}{2}, \frac{5}{2},$  and  $\frac{7}{2}$  for the 1.76-MeV level with the mixing ratios already deduced for these transitions. Acceptable values for  $\chi^2$  below the 0.1% confidence limit are found for all combinations of these spins except for the combination  $J(3.07) = \frac{5}{2}$  and  $J(1.76) = \frac{1}{2}$ . Arguments based on the strength of the observed cross section in the previously reported  $\text{Si}^{30}(t, \alpha)\text{Al}^{29}$  investigation favor a  $J = \frac{5}{2}$  assignment for the 3.07-MeV level. Also, an investigation of the proton angular distribution to this level from a study of the  $\text{Al}^{27}(t, p)\text{Al}^{29}$  reaction investigated<sup>11</sup> at an incident triton energy,  $E_t = 3.5$  MeV, shows that the state is populated by an  $L=0$  two-particle transfer, thus requiring  $J^\pi = \frac{5}{2}^+$  for this state. With this assignment, the correlation of the  $3.07 \rightarrow 1.76$  transition requires  $J(1.76) > \frac{1}{2}$  if  $J(3.07) = \frac{5}{2}$ .

**3.19-MeV level.** The angular distributions of  $\gamma$  rays originating from this level are shown in Figs. 16 and 17. We have carried out simultaneous fits to the  $3.19 \rightarrow 1.76 \rightarrow 0$  transitions, and the  $3.19 \rightarrow 2.23 \rightarrow 0$  transitions. Spin values of  $J = \frac{3}{2}, \frac{5}{2}, \frac{7}{2},$  and  $\frac{9}{2}$  are assumed for the 3.19-MeV level; the anisotropy observed for both the  $3.19 \rightarrow 1.76$ - and  $3.19 \rightarrow 2.23$ -MeV correlations requires  $J > \frac{1}{2}$ . Solutions with  $\chi^2$  below the 0.1% confidence limit can be summarized as follows: If  $J(2.23) = \frac{3}{2}$ , then  $J(3.19) = \frac{3}{2}$  or  $\frac{5}{2}$ ; if  $J(2.23) = \frac{5}{2}$ , then  $J(3.19) =$

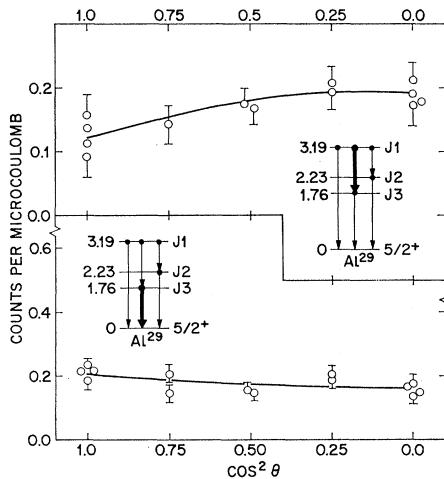


FIG. 16. The angular correlation of  $\gamma$  rays arising from the deexcitation of the 3.19-MeV level. The fits shown to the  $3.19 \rightarrow 2.23$  and  $2.23 \rightarrow 0$   $\gamma$  rays are the result of a least-squares fit of the coefficients of Eq. (1) to the data. The deduced coefficients are given in Table III.

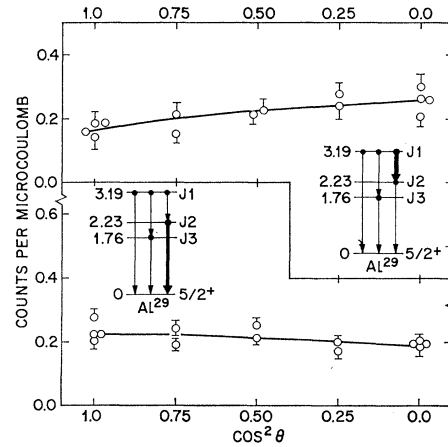


FIG. 17. The angular correlation of  $\gamma$  rays arising from the deexcitation of the 3.19-MeV level. The fits shown to the  $3.19 \rightarrow 1.76$  and  $1.76 \rightarrow 0$  MeV  $\gamma$  rays are the result of a least-squares fit of the coefficients of Eq. (1) to the data. The deduced coefficients are given in Table V.

$\frac{3}{2}, \frac{5}{2},$  or  $\frac{7}{2}$ ; if  $J(2.23) = \frac{7}{2}$ , then  $J(3.19) = \frac{3}{2}, \frac{5}{2}, \frac{7}{2},$  or  $\frac{9}{2}$ . From analysis of the angular correlation of the  $3.19 \rightarrow 1.76 \rightarrow 0$   $\gamma$  rays, all spin values  $\frac{3}{2}$  through  $\frac{9}{2}$  are allowed for the 3.19-MeV state if  $J(1.76) = \frac{5}{2}$  or  $\frac{7}{2}$ . If  $J(1.76) = \frac{3}{2}$  then  $J(3.19) = \frac{9}{2}$  is forbidden and if  $J(1.76) = \frac{1}{2}$  then only  $J(3.19) = \frac{3}{2}$  is allowed. Results for both these levels are summarized in Table IV.

The direct reaction work<sup>1</sup> suggests a tentative assignment of  $\frac{5}{2}^-$  or  $\frac{7}{2}^-$  for this level. The present results do not allow us to add to or modify this assignment.

## V. COLLATION OF RESULTS

The experimental information obtained on  $\text{Al}^{29}$  in this work and in a previous paper is summarized in Fig. 6. We report  $\gamma$ -ray branching ratios for  $\text{Al}^{29}$  levels with  $E_x \leq 3.68$  MeV, and a firm spin assignment  $J = \frac{3}{2}$  for the 2.88-MeV level. Integration of the results from the measurements reported here with previous work results in the possible spin-parity assignments in Fig. 6. Our results agree in essence with other investigations of the nucleus at present in progress.<sup>10,11,13</sup> Discussion of possible differences between these investigations will be left until a later publication.<sup>5</sup> A discussion of the application of a unified model to  $\text{Al}^{29}$ , as well as the results of measurements of the mean lifetimes of some of these levels, will also be presented therein.

<sup>13</sup> D. C. Kean (private communication).